JOURNAL OF OPTOELECTRONICS AND ADVANCED MATERIALS Vol. 8, No. 1, February 2006, 123 - 127

Multiplasmon radiation line replicas of bound excitons in single ZnSe crystals

A. KLYUKANOV*, C. SUSHKEVICI, M. CHYUKICHEV[a], A. AWAWDEH, V. GURAU, A. CATANOI
State University of Moldova, Mateevici 60, Chisinau, 2009 Moldova
[a]*Moscow M. Lomonosov State University, Moscow, 119899 Russia*

The cathode-luminescence of *ZnSe* single crystals, grown from vapour phase and heat treated in *Bi* melts [ZnSe(Bi)] at 1200 *K* for 120*h*, and also in *Bi* melts doped by *Al* [ZnSe(Bi, Al)] were investigated at 4.2 K. The LO-phonon replicas of free excitons emission line dominate in cathode-luminescence spectra of the samples heat treated in *Bi* followed by water quenching. The lines of bound excitons series, $I_1^{s,d} - nLO$, were observed in the emission of all samples, including the original ones. It was found that plasmon replicas are not proper only for $I_1^s - nLO$ lines, but, also, for $I_1^d - nLO$ lines. The weak exciton-plasmon coupling is manifested in one plasmon Stokes side band shoulders of $I_1^d - nLO$ lines. It is developed the theory of bound excitons multi-quantum optical transitions with participation of mixed plasmon-phonon oscillation modes. This theory allows for the calculation of the emission spectra form–function, without using any model. The theoretical spectra are in agreement with the experimental data.

(Received October 14, 2005; accepted January 26, 2006)

Keywords: Cathodo-luminescence, ZnSe single crystal, Bound exciton lines, Multi-quantum optical transition

1. Introduction

The particularities of bound excitons emission spectra determined by exciton coupling with LO-phonons and plasmons at 4.2 K were analysed in the papers [1-3], where the cathode-luminescence of *ZnSe* single crystals, heat treated in vacuum and also in Zn, Sb and Bi melts were investigated.

Bound excitons emission spectra series $I_1^s - nLO - mPl$ exhibiting strong coupling with LO- phonons and plasmons have a phononless band I_1^s at 456 nm. The interaction between I_1^s bound excitons and mixed lattice-plasma oscillations manifests itself in multiplasmon structure of spectra. Strong exciton-phonon coupling originates from the I_1^s centre nature due to unequal localization radii of electron and hole staxes. It was found, that for comparative high concentration of free electron - $N \approx 10^{17}$ cm^{-3}, when the mixing of LO-phonons with plasmons takes place, the constants of bound exciton coupling with LO-phonons N_{LO} and plasmons N_p, and also the energetic distances between the satellites in $I_1^{s,d} - nLO - mPl$ series lines depend on the free carrier plasma concentration *N* [2]. The resonance interaction of bound I_1^s and I_1^d excitons with up mode of mixed plasmon-phonons oscillations leads to the I_1^d line (445,8 nm) splitting, like pinning [3].

This work is devoted to far investigations of multiplasmon structure of $I_1^{s,d} - nLO$ lines.

We have to mention, at first, that the theory of bound exciton emission spectra shape was developed in works [1-3], using the well-known Vannier-Mott approximation. In this paper we examine the bound exciton emission spectra form-function without using any model approximation. The starting point for our consideration is the Heisenberg equation of motion for microscopic polarisation operators with taking into account the unscreened Coulomb interaction within the many-body electrons and nucleus system.

2. Multi-quantum optical transitions

The response under the external longitudinal and transversal electromagnetic fields of many-body system with the Hamiltonian

$$\hat{H} = \sum_{\alpha,n,m} \hat{h}_{nm}^{\alpha} \hat{a}_{n\alpha}^{+} \hat{a}_{m\alpha} + \frac{1}{2} \sum_{\kappa,\alpha} V_{\kappa}^{\alpha\alpha} \sum_{m,n,l,p} e_{l,n}^{i\kappa r_{\alpha}} e_{p,m}^{-i\kappa r_{\alpha}} \hat{a}_{l\alpha}^{+} \hat{a}_{p\alpha}^{+} \hat{a}_{m\alpha} \hat{a}_{n\alpha} \qquad (1)$$

$$V_{\kappa}^{\alpha\beta} = \frac{4\pi q_{\alpha} q_{\beta}}{V\kappa^2}$$

is given by the time dependence of the microscopic polarisation operator [1-6]:

$$\hat{P}_{if}^{\alpha} = \hat{a}_{i\alpha}^{+} \hat{a}_{f\alpha} \ , \ \frac{\partial \hat{P}_{if}^{\alpha}}{\partial t} = \frac{i}{\hbar} \left[\hat{H}, \hat{P}_{if}^{\alpha} \right] \qquad (2)$$

Here $\hat{a}_{i\alpha}^{+}$, $\hat{a}_{f\alpha}$ are the creation and destruction operators, $V_{\kappa}^{\alpha\beta}$ is the Fourier transform of Coulomb potential. The i, f subscripts represent the quantum numbers sets, describing the many-body system eigen-

functions. The $\alpha = e, n$ ($q_e = e$) index distinguishes electrons and nuclei. The interaction with electromagnetic field and Coulomb attraction between electrons and nuclei are included in the operator

$$\hat{h}^{\alpha} = \frac{1}{2m_{\alpha}}(\hat{p}_{\alpha} - \frac{q_{\alpha}}{c}\hat{A}_{\alpha}(r_{\alpha},t))^2 + q_{\alpha}\varphi(r_{\alpha},t) + \sum_{\beta}{}' \sum_{\kappa} V_{\kappa}^{\alpha,\beta} e^{i\kappa r_{\alpha}} \hat{\rho}_{\kappa}^{\beta} \quad (3),$$

$$\hat{\rho}_{\kappa}^{\beta} = \sum_{n,m} e_{nm}^{-i\kappa r_{\beta}} \hat{P}_{nm}^{\beta}$$

where $\hat{p}_{\alpha}$ is the momentum operator, r_{α} is the radius vector of particle with charge q_{α}. Other notations are standard.

The solution of Heisenberg equation of motion (2) for the operator $\hat{P}_{if}$, with the calculation of the commutators and transforming the four operator terms, can be presented as (index α is temporarily omitted)

$$\frac{\partial \hat{P}_{if}}{\partial t} = i\hat{\omega}_{if} P_{if},$$

$$\hat{P}_{if}(t) = T\exp\left\{ i\int_0^t \hat{\omega}_{if}(s)ds \right\} \hat{P}_{if}(0) \quad (4)$$

Here T is the symbol of chronological time-ordering, and $\hat{\omega}_{if}$ is the operator of transition frequency, determined by the expression:

$$\hbar\hat{\omega}_{if} = \hbar\hat{\omega}_{if}^{HF} + \hat{\tilde{h}}_{fi}(1-\delta_{fi})\hat{C}_{fi} + \sum_{n}^{i,f}(\hat{\tilde{h}}_{ni}\hat{C}_{ni} + \hat{\tilde{h}}_{fn}\hat{C}_{fn}) \quad (5)$$

The symbols i, f in the sum after n mean that the terms with $n = i, f$ have to be excluded. The first term in equation (5) determines the diagonal part of the operator of transition frequency $\hat{\omega}_{if}^{HF}$ in the generalised Hartree-Fock approximation:

$$\hbar\hat{\omega}_{if}^{HF} = \hat{E}_i - \hat{E}_f - \sum_{\kappa} V_{\kappa} M_{ff}^{ii}(\hat{P}_{ff} - \hat{P}_{ii}) + \\ + \sum_{\kappa} V_{\kappa}\left(\sum_{n}^{i} M_{in}^{ff}\hat{P}_{in} - \sum_{n}^{k} M_{nf}^{ii}\hat{P}_{nf} \right) \quad (6)$$

$$M_{nm}^{kl} = e_{nm}^{i\kappa r} e_{kl}^{-i\kappa r} - e_{nl}^{i\kappa r} e_{km}^{-i\kappa r},$$

$$\hat{E}_i = \hat{h}_{ii} + \sum_{\kappa} V_{\kappa} \sum_{nm} M_{nm}^{ii}\hat{P}_{nm}$$

The non-diagonal terms in theequation of motion (2) are turned to diagonal form (4), using the commutation operators $\hat{C}_{nm}$. The commutation operator action upon the micro-polarisation operator $\hat{P}_{if}$, according to the definition, consists of

$$\hat{C}_{nm}\hat{P}_{if} = [\hat{P}_{nm}, \hat{P}_{if}] = \hat{P}_{nf}\delta_{im} - \hat{P}_{im}\delta_{nf} \quad (7)$$

Berezin has examined in [7] the commutation operator of equation of motion (2). The explicit cumbersome form of the expressions for operators $\hat{\tilde{h}}_{mn}$ in equation (5) will be not presented here.

The calculation of microscopical response under external perturbations includes the operation of quantum statistic averaging with the use of the equilibrium density matrix. Taking into account the approximation $\hbar\hat{\omega}_{if} = \hbar\hat{\omega}_{if}^{HF}$, then, by expanding T exponent (4) in series and carrying out the operation of decoupling and averaging we obtain:

$$\hat{P}_{if}(t) = G_{if}(t)\hat{P}_{if}(0),\ G_{if}(t) = \exp\left(i\int_0^t \langle\hat{\omega}_{if}(s)\rangle ds + g_2(t) \right) \quad (8)$$

$$g_2(t) = -\int_0^t ds \int_0^s ds_1 \left\{ \langle\hat{\omega}_{if}(s)\hat{\omega}_{if}(s_1)\rangle - \langle\hat{\omega}_{if}(s)\rangle\langle\hat{\omega}_{if}(s_1)\rangle \right\}$$

This result for micro-polarization operator corresponds to taking into consideration of two first terms in cumulant expansion method [8]. As it is known, the random phase approximation supposes the replacement of instantaneous field created by plasma, with averaging [9]. The micro-polarization operator (8), calculated in the same approximation of the average transition frequency, can be used next for evaluation of the response function, the light absorption coefficient and the spontaneous recombination rate. The first order cumulant is

$$\langle\hbar\hat{\omega}_{if}\rangle = \langle\hat{E}_i - \hat{E}_f\rangle - \sum_{\kappa} V_{\kappa} M_{ff}^{ii}(n_f - n_i),\ n_f = \langle\hat{P}_{ff}\rangle, \quad (9)$$

Beside the Hartree-Fock difference of proper energies $\langle\hat{E}_i - \hat{E}_f\rangle$ of initial i and final f states (Cumans approximation), Eq. (9) takes into account the unscreened Coulomb interaction between the quasi-particle in f state and quasi-hole in i state. The second order cumulant is:

$$g_2(t) = -\frac{1}{\hbar^2}\int_0^t ds \int_0^s ds_1 \sum_{\kappa} (V_{\kappa}^{\alpha})^2 \left| M_i^f \right|^2 \langle\hat{\rho}_{\kappa}(t_1)\hat{\rho}_{-\kappa}(t_2)\rangle, \quad (10)$$

$$M_i^f = e_{ii}^{i\kappa r_{\alpha}} - e_{ff}^{-i\kappa r_{\alpha}}$$

and describes the effect of exciton Coulomb interaction screening and multi-quantum transitions. We express the correlator density-density from equation (9) through the longitudinal dielectric function, using the fluctuation-dissipation theorem [9]. The second cumulant has the following expression

$$g_2(t) = \frac{1}{\pi\hbar}\sum_{\kappa} V_{\kappa} \int_{-\infty}^{\infty} dv (n_v + 1) \mathrm{Im}\left\{ \frac{1}{\varepsilon^*(\kappa, v)} \right\} \left| M_i^f \right|^2 [it + \frac{1}{v}(e^{-ivt} - 1)], \quad (11)$$

$$n_v = \frac{1}{e^{\beta v} - 1},\ \beta = \frac{\hbar}{k_0 T}$$

The linear term with respect to time *t* contribution in g_2 (11) can be transformed using the sum rule

$$\int_{-\infty}^{\infty} \frac{dv}{v}(n_v + 1)\,\mathrm{Im}\{\frac{1}{\varepsilon^*(\kappa, v)}\} = \int_0^{\infty} \frac{dv}{v}\,\mathrm{Im}\{\frac{1}{\varepsilon^*(\kappa, v)}\} = \frac{\pi}{2}\{1 - \frac{1}{\varepsilon(\kappa,0)}\} \quad (12)$$

Expressions (8-12) show that the exciton Coulomb interaction screening is determined by the static dielectric function $\varepsilon(\kappa,0)$ [10]. In the similar manner, taking into account the operator $\hat{\hat{h}}_{fi}$ (5) in the second order cumulant approximation, one can get that the exciton exchange interaction screening is dynamic [11]. The obtained results [1-3] consist in the expansion at the arbitrary degeneration case in many-body systems. The second order cumulant (11), beside the screening effect [10, 11], describes the multi-quantum emission and absorption processes of elementary excitations. Their frequencies can be determined from the equation $\varepsilon(\kappa,\omega)$=0. The lattice and plasma band charge carrier dynamics determine the exciton coupling with mixed plasmon-phonons modes [2, 9]. At low temperatures ($k_0T << \hbar\omega_{LO}$), the *LO* - phonon structure of bound exciton emission spectra in the harmonic approximation (dielectric function has the first order singularity in the point $v = \omega_{LO}$) has to obey the Poisson distribution for the lines intensities, according to equation (11). The spectra shape is described by the superposition of Lorenz functions [1-3]. Their parameters (interaction constants N_{LO} and N_p, peak line positions and their half-widths) are calculated in this work from equations (8-11), without using the Vanier-Mott approximation, as distinct from results of works [1-3]. Here, we determine them by comparing the theory with experimental data.

3. Experimental results and discussion

The cathode-luminescence spectra of ZnSe single crystals have been excited by electron beam with energy - 40keV , at 4.2K . The impulse duration was $40\mu s$ and their frequency - 200Hz . The spectra detection was carried out with single-grating monochromator in the spectra visual region. ZnSe single crystals, grown from vapour phase, heat-treated in vacuum and also in *Bi* and *Bi* $+10^{-3}$ at. % Al melts at 1200 *K* for 120*h*. The quenching was realised by ampoule dipping in water. In Fig. 1 are presented experimental results of cathode-luminescence spectra of ZnSe crystals heat treated in *Bi* melts followed by water quenching (curve 1), in *Bi* melts doped *Al* [ZnSe(Bi, Al)], curve 2 and untreated original crystal, curve 3. LO- phonon replicas of free excitons emission line were observed in samples heat treated in *Bi* with following water quenching (curve 1) and also in crystals [ZnSe(Bi, Al)] (curve 2). Emission $I_1^d - nLO$, as it is known, arises from the radiative recombination of an exciton bound to V_{Zn} (I_1^d exciton). As it is shown (curve 1 in Fig. 1), the free exciton LO -phonon replicas ($Ex - nLO$) dominate the $I_1^d - nLO$ lines series of bound to V_{Zn} exciton in [ZnSe(Bi)] crystals. The free and I_1^d bound exciton coupling with LO-phonons is weak ($N_{LO} \cong 0{,}2$ for I_1^d exciton). Here N_{LO} is the mean phonons number at one emitted photon. On the contrary, $I_1^d - nLO$ series dominates in [ZnSe(Bi, Al)] crystals and LO -phonons replicas of free exciton line $Ex - nLO$ are exhibited as a side band Stokes shoulders of I_1^d and $I_1^d - LO$ lines, curve 2 in Fig. 1. This fact is caused the V_{Zn} concentration increasing in [ZnSe (Bi , Al)] crystals, in comparison with ZnSe crystal heat treated in *Bi* with following water quenching. The relative lines intensity in Fig. 1 (curve1 and 2) is the same. Spectrum 2 can be obtained from 1 if just to increase the I_1^d centre

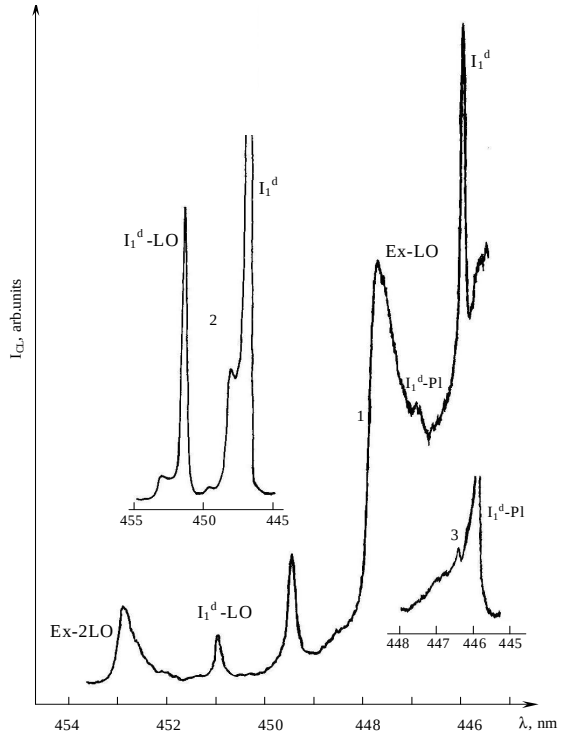

Fig. 1. The cathode-luminescence spectra of ZnSe crystals at T=4.2K. 1 – sample heat treated in Bi melts with following water quenching, 2- sample ZnSe (Bi, Al), 3- the original untreated sample grown from vapour phase.

concentration with regard to the radiative recombinated free excitons concentration. Curve 3 in Fig. 2, representing the original ZnSe crystal emission spectrum, is not in conformity with this knowledge. It cannot be obtained from spectrum 1. If we assume that the shoulders on I_1^d

and $I_1^d - LO$ lines on curve 3 in Fig. 2, represent one- and bi- LO -phonons replicas $Ex - LO$ and $Ex - 2LO$ of free exciton emission line, then the intensity of $Ex - 2LO$ line ($\lambda = 452\,nm$) has to be bigger twice. In works [3,12] the $I_1^d - nLO$ lines side band shoulders are assigned to the radiative recombination with acoustic phonons, free excitons and plasmons involving participation in the emission. Acoustic phonons could be excluded from the consideration first. Indeed, the lattice dynamic determinates the acoustic oscillations and they have to manifest themselves in emission spectra of all samples. However, in some original $ZnSe$ samples these side band shoulders do not appear, as it is shown in Fig. 2, curve 1. The origins of these shoulders can be assigned to LO-phonon replicas $Ex - nLO$, or to one-plasmon replicas $I_1^d - nLO - Pl$. Indeed at low plasma concentration ($N < 10^{16} cm^{-3}$), the interaction with conduction band electrons plasma is not exhibited in accordance with experiment, as it is shown in Fig. 2, curve 1.. The distinguishing of free exciton $Ex - nLO$ and plasmon $I_1^d - LO - Pl$ is more difficult.

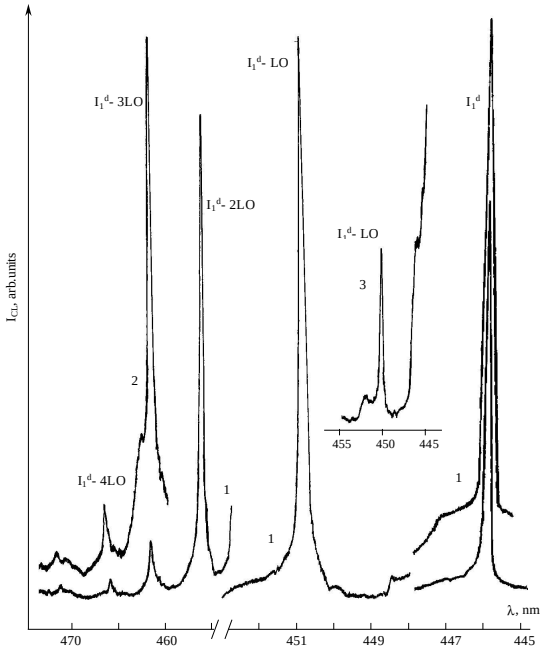

Fig. 2. The cathode-luminescence spectra of $ZnSe$ crystals at low plasma concentration $\omega_p < \omega_{LO}$, 1,3- two original samples, 2- sample heat treated in Bi.

The excitons participation in the emission of $ZnSe$ crystals, heat treated in *Bi* with following water quenching, presented in Fig.1, curve 1, is undoubted, but it is more difficult to determinate the shoulder nature of lines on curve 2 in Fig. 1 and 3 in Fig. 2. However, one can assume that the shoulders of lines on curve 2 in Fig. 1 are the LO-phonon replicas of free exciton emission $Ex - nLO$ and on curve 3 in Fig. 2 are the plasmon replicas $I_1^d - Pl$ and $I_1^d - LO - Pl$. The difference of the studied lines relative intensities and their spectral peak positions indicate this fact. In accordance with experimental data, the plasmon replicas peaks are situated closer to $I_1^d - nLO$ lines, then excitons ones. So, $Ex - 2LO$ line has emission maximum at $\lambda = 453\,nm$ (curve 2 in Fig. 1), but $I_1^d - LO - Pl$ line at $452.5\,nm$ (curve 3 in Fig. 2). If the electron temperature increases, $Ex - nLO$ lines maxima shift in short wave spectra region at unchangeable long-wave edge positions. However, it leads to the broadening of the lines $Ex - nLO$. Hence, the narrow shoulders of lines I_1^d on curves 3 in Fig. 2 and $I_1^d - LO$ in Fig.1 are the plasmon replicas $I_1^d - Pl$ and $I_1^d - LO - Pl$.

The plasmon replica $I_1^d - Pl$ of I_1^d line is the most evident on curve 1 in Fig.1, where it is situated between $Ex - LO$ and I_1^d lines ($\hbar\omega_p = 6\,meV$).

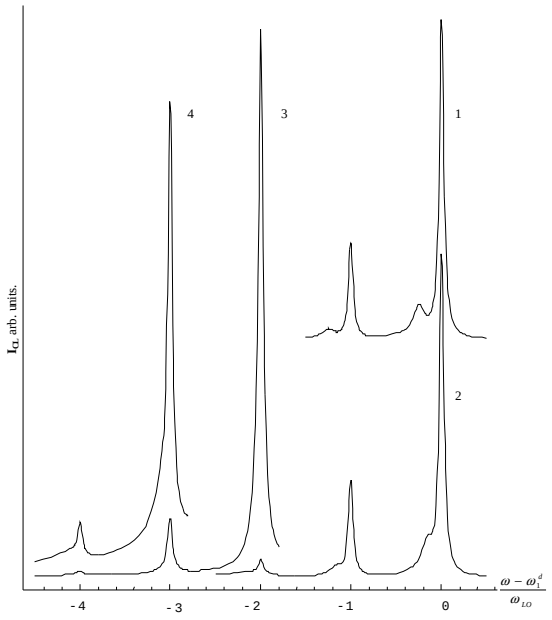

Fig. 3. The $I_1^{s,d} - nLO - mPl$ lines emission bands shape calculated using equation (4), work [1]. Spectra were obtained at the next N parameters values $N_{LO}^d = 0.3$, $N_p^d = 0.25$, $N_{LO}^s = 1.5$, 1 - $\omega_p = 0.25\,\omega_{LO}$, $N_p^s = 2$; 2 - $\omega_p = 0.16\,\omega_{LO}$, $N_p^s = 2$; 3 - $\omega_p = 0.05\,\omega_{LO}$, $N_p^s = 2.8$. The band intensities ratio 1,2 - $I_1^d : I_1^s$ = 64:1; 3 – 6400:1.

At low concentration, the bound exciton coupling with plasma leads to the broadening of the $I_1^{s,d} - nLO$ lines. However, as the concentration grows to N~ 10^{17} cm^{-3} the broadening is replaced by a narrowing of the

$I_1^{s,d} - nLO$ lines. If the electrons concentration in conduction band is high sufficient that plasmon replicas could split off from $I_1^{s,d} - nLO$ lines, then their half-width becomes smaller. This behaviour is characteristic for $I_1^s - nLO$ series more (see Fig. 1 [2] work) and less for $I_1^d - nLO$ lines. The theoretical calculation results of bound exciton emission spectra in $ZnSe$ crystals at various energy of low-frequency plasmons $\hbar\omega_p$, taking into account the superposition of $I_1^s - nLO - mPl$ and $I_1^d - nLO - mPl$ lines, are presented in Fig. 3. The superposition can be exhibited not only in I_1^s and $I_1^d - 2LO$ (456 nm, x= -2) [2] region, but in the next LO-phonon replicas regions too, in dependence of I_1^s and I_1^d lines relative intensity. These emission spectra particularities are in accordance with experimental data, presented in Fig. 2, curves 1,2, in wavelength region $456 - 472nm$. Strong coupling of I_1^s bound exciton with plasmons ($N_p^s > 1$) leads to the broadening of series lines $I_1^s - nLO$ ($N_{LO}^s = 1.4, N_p^s = 2$) and the narrow $I_1^d - (n+2)LO$ lines are superposed with them. This superposition is observed in Fig. 2, curves 1,2. The superposition of $I_1^s - LO$ and $I_1^d - 3LO$, $I_1^s - 2LO$ and $I_1^d - 4LO$, $I_1^s - 3LO$ and $I_1^d - 5LO$ lines manifest themselves at $\lambda = 461nm$, $\lambda = 467nm$, $\lambda = 472$ nm accordingly.

The agreement of theory with experiment is satisfactory.

4. Conclusions

The cathode-luminescence of *ZnSe* single crystals, grown from vapour phase and heat treated in *Bi* melts [ZnSe(Bi)] at 1200 *K* for 120 *h*, and also in *Bi* melts doped by *Al* [ZnSe(Bi, Al)] were investigated at 4.2 K. The LO-phonon replicas of free excitons emission line dominate in cathode-luminescence spectra of the samples heat treated in *Bi* followed by water quenching.

It is developed the theory of bound excitons multi-quantum optical transitions with participation of mixed plasmon-phonon oscillation modes. This theory allows for the calculation of the emission spectra form–function, without using any model. The theoretical spectra are in agreement with the experimental data.

References

[1] V. S. Vavilov, A. A. Klyukanov, K. D. Sushkevich, M. V. Chukichev, A. Z. Awawdeh, R. R. Rezvanov, Fiz. Tverdogo Tela (russ.) **41**(7), 1176 (1999).

[2] V. S. Vavilov, A. A. Klyukanov, K. D. Sushkevich, M. V. Chukichev, A. Z. Awawdeh, R. R. Rezvanov, Fiz. Tverdogo Tela (russ.) **43**(5), 776 (2001).

[3] A. A. Klyukanov, K. D. Sushkevich, M. V. Chukichev, V. Gurau, Fiz. Tverdogo Tela (russ.) **46**(10), 1746 (2004).

[4] V. M. Agranovich, Teoria exitonov (russ.), Nauka, M. (1965).

[5] Y. Toyozawa, Progr. Theor. Phys. (Kyoto) **27**(1), 89 (1962).

[6] F. P. Bassani, D. P. Parravichini, Electronnie Sostoiania I Opticheskie Perehodi v Tverdih Telah (Electron states and optical transitions in solid state), (russ.) Nauka, M. (1968).

[7] F. A. Berezin, Metod Vtorichnogo kvantovania (Method of second quantification), (russ.) Nauka, Moscow (1965).

[8] R. Y. Kubo, Phys. Soc. Japan **17**(7), 1100 (1962).

[9] P. M. Platsman, P. A. Wolf, Waves and Interactions in Solid State Plasmas, New York: Academic, 1973.

[10] S. D. Mahanti, C. M. Varma, Phys. Rev. **B6**, N6, 2209 (1972).

[11] V. A. Kisilev, A. G. Jilich, Fiz. Tverdogo Tela (russ.) **14**, 1438 (1972).

[12] J. L. Merz, H. Kukimoto, K. Nassau, J. W. W. Shiever, Phys. Rev. B **6**(2), 545 (1972).

* Corresponding author: klukanov@usm.md